Journal of the European Ceramic Society **13** (1994) 285–291

Synthesis and Characterization of Nanocomposite Si/C/N Powders by Laser Spray Pyrolysis of Hexamethyldisilazane

Nathalie Herlin, Michel Luce, Emmanuel Musset & Michel Cauchetier

CEA–DSM–DRECAM, Service des Photons, Atomes et Molécules, CE Saclay, 91191 Gif-sur-Yvette Cedex, France

(Received 27 May 1993; revised version received 30 October 1993; accepted 2 November 1993)

Abstract

Ultrafine amorphous Si/C/N powders are obtained using ultrasonic injection of a liquid precursor (hexamethyldisilazane: HMDS) into the beam of a high power industrial cw-CO_2 laser. Up to 100 cm^3/h of liquid are displaced with a conversion efficiency (liquid→powder) of about 45%. The chemical composition is controlled by varying the synthesis conditions. Nitrogen-rich powders are produced by adding ammonia in the reaction zone. These pre-ceramic powders are nanosized and monodispersed. The improvements due to the use of liquid precursors are discussed (in particular safety). The effect of annealing under nitrogen atmosphere has been studied by various diagnostics (chemical analysis, BET, XRD).

Ultrafeine amorphe Si/C/N Pulver konnten durch Ultraschalleinspritzung einer flüssigen Vorstufe (Hexamethyldisilazane: HMDS) in den Strahl eines industriellen Hochleistungs-CO_2-Lasers erzeugt werden. Der Durchsatz betrug 100 cm^3/h einer keramischen Ausbeute (HMDS→Pulver) von ca. *45%. Dabei kann die chemische Zusammensetzung des Pulvers durch Veränderung der Synthesebedingungen kontrolliert werden. Stickstoffreichere Pulver konnten durch Zufuhr von Ammoniak in den Reaktionsbereich gewonnen werden. Diese nanometrischen präkeramischen Pulver weisen sehr enge Korngrößenverteilungen auf. Die Verbesserungen aufgrund der Verwendung eines flüssigen Vorproduktes werden diskutiert insbesondere die Sicherheit des Verfahrens. Der Effekt des Aufheizens unter Stickstoffatmosphäre ist mit verschiedenen Diagnoseverfahren (chemische Analyse, BET, XRD) untersucht worden.*

Des poudres ultrafines, amorphes de composition Si/C/N ont été obtenues par injection ultrasonique d'un précurseur liquide (hexaméthyldisilazane: HMDS) dans le faisceau d'un laser industriel CO_2 continu de forte intensité. On peut déplacer à l'échelle du laboratoire jusqu'à 100 cm^3/h de liquide avec un taux de conversion (liquide→poudre) de l'ordre de 45%. La composition chimique des poudres est controlée en faisant varier les conditions de synthèse. Des poudres riches en azote sont obtenues en ajoutant de l'ammoniac dans la zone de réaction. Ces poudres pré-céramiques sont de taille nanométrique et monodisperses. Les progrès dus à l'emploi de précurseurs liquides sont discutés (en particulier la sécurité). L'effet du recuit sous atmosphère d'azote a été étudié par différents types de diagnostic (analyse chimique, BET, RX, IR).

1 Introduction

Materials with novel properties are obtained when the constituent phase morphology is reduced to nanometer dimensions.[1] A significant improvement in thermomechanical properties can be achieved by the use of homogeneous nanophase powders for various compositional systems (for example, Si/C/N). The growing interest in Si/C/N nanocomposite ceramics is also explained by their large range of properties from superplastic[2] to a high strength and toughness, depending on the composition. The performances of the final products are strongly affected by the properties of the original powders, therefore the synthesis of the pre-ceramic powders must be carefully controlled.

Silicon carbonitride ceramics or Si/C/N pre-ceramic powders can be synthesized by various processes: some examples are now given. Almost ten years ago, mixtures of Si_3N_4, SiC and C were produced from the pyrolysis of pre-ceramic polyorganosilazanes.[3] Si_3N_4 + SiC mixed powders

Journal of the European Ceramic Society 0955-2219/94/$7.00

have also been synthesized in a plasma system.[4] Fine amorphous Si/C/N powders have been obtained from vapour phase reaction of organosilicon compounds.[5] Nanostructured Si/C/N powders have been obtained by injection of a precursor aerosol into a hot wall reactor.[6] Compared to these methods, the laser-induced synthesis offers several advantages. Due to the coherent beam, the chemical reaction zone is very well defined and there is no possibility of chemical interaction with the walls. The ability of this method to produce spherical, ultrafine and high purity ceramic powders with a controlled size and chemical composition[7] has already been demonstrated. Powders containing silicon, nitrogen and carbon have already been obtained from the interaction of a CO_2 laser with different mixtures, usually silane (SiH_4) and nitrogen organic compounds.[8-10] However, silane is an expensive and hazardous gas. In order to scale up the process with increased safety, nitrogeneous organosilicon compounds are preferred.[11]

This paper reports on the synthesis of Si/C/N preceramic powders, using as precursor a mixture of an aerosol of hexamethyldisilazane (HMDS) and ammonia (NH_3). Among the different experimental parameters (irradiation geometry, laser power, pressure, etc.), the influence of reactant composition and residence time on the final product has been studied. The aim is to control the chemical composition of the products through the choice of experimental conditions. The results of annealing experiments are also presented. The evolution of the structure and the crystallization is studied as a function of temperature.

2 Experimental

The experimental device is described elsewhere.[12] The salient features related to the present experiment are now briefly listed. The liquid precursor hexamethyldisilazane (HMDS, $((CH_3)_3Si)_2NH$) is manipulated without any special care. Before an experiment, it is placed in a special glass jar containing a piezoelectric transducer (Pyrosol 7901 type from RBI) with bubbling argon. After a few minutes under flowing argon, an intense beam of ultrasound is focused near the free surface of the liquid, generating a fountain which leads to an aerosol. The aerosol droplets are carried out by a flow of argon via a glass tube of variable inner diameter which serves as an inlet into the beam of a high powered CO_2 laser (CI 1000 from CILAS). The unfocused laser beam (maximum power = 1 kW) is expanded ($\times 2$); the beam diameter is then 25 mm. The powders presented here are obtained with a constant laser power: 600 W (120 W/cm^2 power density). The infrared spectrum of HMDS has a strong absorption band in the region of the emission wavelength of the CO_2 laser at 10·6 μm.[13] The strong interaction between the laser beam and the precursor droplets results in the rapid formation of pre-ceramic powders. The irradiation cell operates under a regulated pressure of 760 torr very similar to those previously described.[8] The powders are collected in a glass chamber equipped with a cylindrical metallic filter heated at about 120°C. After collection, the powders are preserved in a glove box. The pellets used in annealing experiments are made and manipulated in air without any special care. Heating treatments under flowing N_2 are performed at atmospheric pressure in a high-temperature graphite furnace (GE 80 model from Pyrox) at various temperatures between 1000 and 1600°C. A heating rate of 670°C/h and a dwell time of 1 h at the set temperature are used.

The products (as-formed and annealed) are characterized by different methods:

- —Conventional chemical analysis conducted by the CNRS analysis laboratory.
- —IR spectroscopy using the KBr pellet technique.
- —Transmission electronic microscopy (TEM, CM 20 Philips, 200 keV).
- —Thermogravimetric analysis (TGA) performed by CEA or by Elf-Atochem.
- —Nitrogen absorption–desorption (Brunauer, Emmet, Teller method). BET surface areas are measured using a Micromeritics Flowsorb-2300.
- —The evolution of the structure is followed by X-ray diffraction. X-Ray diffraction diagrams are obtained using Cu-K_α radiation.

3 Results and Discussion

3.1 Synthesis

Table 1 presents the main experimental parameters of the synthesis and the production results. The mean conversion efficiency liquid → powder is about 40%, substantially lower than the 70% obtained by Gonsalves *et al.*[11] In the present authors' earliest experiments, the powder production rate was quite slow (8·7 g/h in HMDS 02, Table 1). Due to better irradiation conditions, the powder production rate is now most often in the range 25 to 38 g/h, a third of the production rate (100 g/h) previously claimed[11] though the time of operation is not known. The Si content in the precursor used by Gonsalves *et al.*[11] is 47 wt% compared to 35 wt% in HMDS, which partially explains the lower production rate obtained in the present experiment. The present

Table 1. Experimental parameters and production results

Run	*Ar flow* (cm^3/min)	NH_3 *flow* (cm^3/min)	*Nozzle diameter* (*mm*)	*Powder weight* (*g/h*)	*Conversion rate* (%)
HMDS 22	1900	0	9	22	34
HMDS 25	2060	0	9	28	46
HMDS 26	2120	0	9	32	45
HMDS 27	2185	0	13	27	39
HMDS 28	2640	0	13	38	46
HMDS 29	2660	275	13	30	38
HMDS 31	2080	725	13	28	47
HMDS 32	2660	140	13	28	43
HMDS 35	2350	1000	13	21	32
HMDS 02	710	520	9	8·7	—
HMDS 06	1200	620	9	14·8	—

experiment is stable for more than one hour and the resultant quantity of powder is then sufficient to perform annealing experiments. The maximum amount of powder was obtained for HMDS 26—44 g in 82 min.

At a temperature of about 115°C, the vapour pressure of HMDS is sufficient to introduce HMDS into the reactor in the vapor phase.[13] In such a configuration, the conversion efficiency is higher but the weight of displaced liquid is lower than in the previous case and the maximum powder production rate is much lower—a few g/h.

3.2 Powder characterization

Table 2 shows that the BET specific surface area depends on the residence time of the reactants in the interaction zone for the powders obtained from pure HMDS (HMDS 22 to 28). The measured surface area increases with the linear speed of the reactants passing in the interaction zone. There is no such clear relation with NH_3 (HMDS 02, 06, 29–35). This is related to turbulence appearing in the flame when NH_3 is added to the reaction.

Chemical analysis shows that the O content is less than 10 wt% for powders preserved in a glove box under an argon atmosphere but later on manipulated in air without any special care, which is low compared to other works[9]—18–26 wt%. Clearly, this difference is due to the lower power laser (50 W) used by these authors.[9] Nevertheless, the sample HMDS 06, which was stored in air for more than one year, shows the high sensitivity of these powders towards oxidation. The Si content remains stable in the amorphous powders ($\approx$48 wt%), through a large variety of experimental conditions. The silicon yield (liquid → powder) is then calculated to be around 60% in all the experiments presented here. It can also be interesting to follow the evolution of C and N contained in the powders as a function of experimental conditions. Table 2 shows that quite different C/N values may be obtained by the present synthesis method ($0{\cdot}2 < C/N < 2{\cdot}5$). The C/N ratio in the solid phase and in the precursor mixture are closely related, as seen in Fig. 1(a). Figure 1(b) shows that the wt% of C in the powder varies almost linearly with the wt% of C in the reactant phase ($30\% < C_{reactant} < 50\%$). These observations show that the control of the chemical composition of the product can be easily achieved through manipulation of the precursor mixture.

The powders produced are always amorphous and often nanodispersed, as indicated by TEM micrographs. For example, in the case of HMDS 22 (Fig. 2), the mean diameter is 40 nm and the size

Table 2. Characterization of pre-ceramic powders

Run	*Linear velocity* (*m/s*)	S_{BET} (m^2/g)	*C/N ratio*	*C* (*wt%*)	*N* (*wt%*)	*Si* (*wt%*)	*O* (*wt%*)
HMDS 22	0·50	139	2·2	28	13	49	9
HMDS 25	0·54	116		29			
HMDS 26	0·56	132		29			
HMDS 27	0·27	82					
HMDS 28	0·33	88	2·5	30	12	50	6
HMDS 29	0·33	167	1·4	24	17	48	8
HMDS 31	0·26	116	0·8	19	23	48	6
HMDS 32	0·33	95	1·4	25	18	48	7
HMDS 35	0·42	144	0·2	7	33	47	10
HMDS 02	0·32	101	0·2	6	31	48	8
HMDS 06	0·48	136	0·3	7	22	48	18

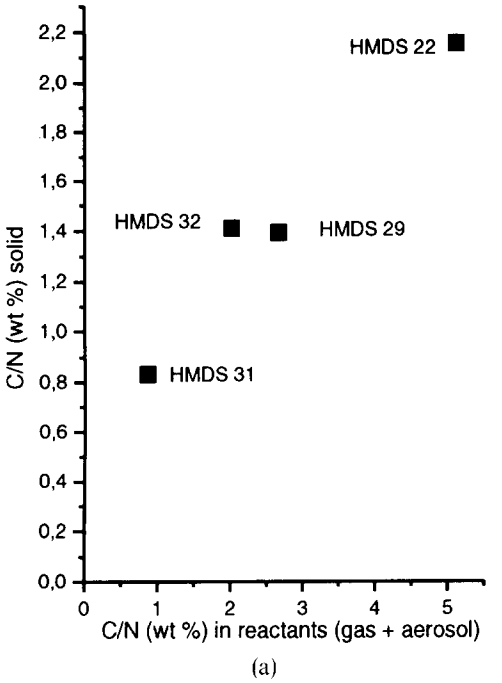

(a)

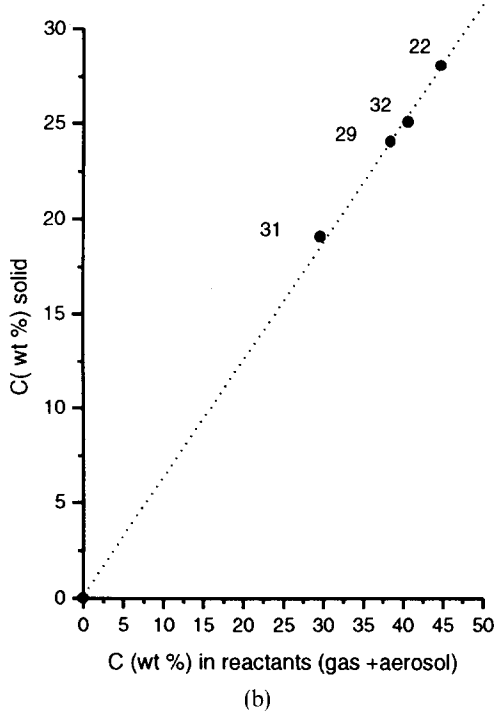

(b)

Fig. 1. (a) Evolution of C/N content in the powders as a function of C/N content in the reactants. (b) Evolution of C content in the powders as a function of C content in the reactants. The dotted line ($C_{powder} = 0{\cdot}6 \times C_{reactant}$) has been added as a guide for the eyes.

distribution is rather narrow: 70% of the particles have a diameter between 36 and 48 nm. For HMDS 31, a bimodal distribution is observed (Fig. 2).

IR analysis of HMDS 22 to 28 shows unambiguously the presence of N–H, Si–H, C–H, and Si–CH_3 bonds. A broad band between 1100 and 800 cm^{-1} is usually attributed to Si–C, Si–O and N–H. The spectrum is very similar to that presented in Ref. 11. The relative intensity of the peaks shows that HMDS 22 is more hydrogenated than HMDS 25–28. For powders obtained by adding NH_3

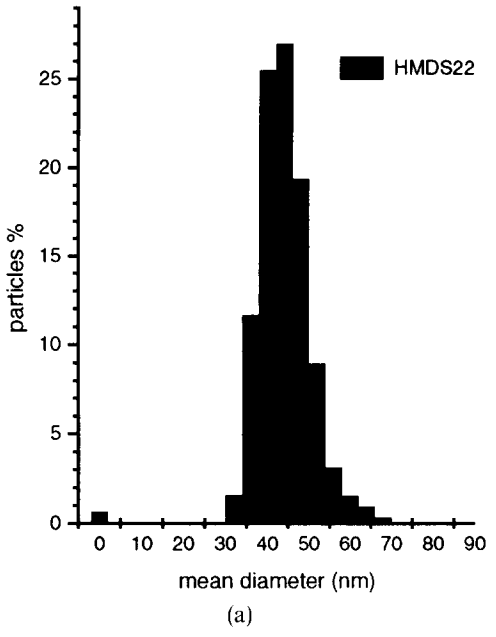

(a)

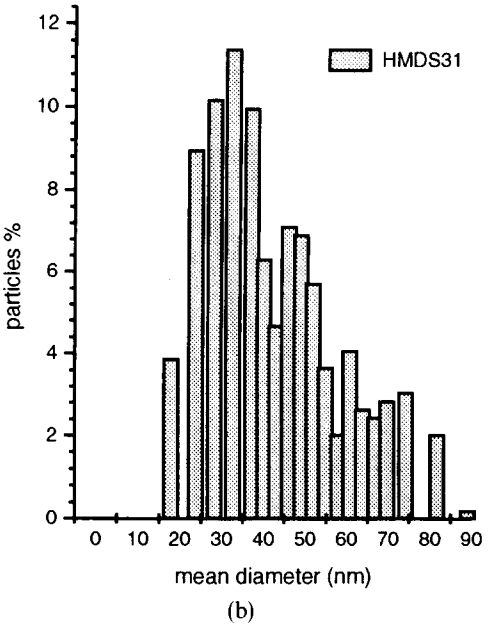

(b)

Fig. 2. Size distribution of samples (a) HMDS 22 and (b) HMDS 31.

(HMDS 02, 06, 29–35) in the precursor mixture, i.e. N-rich powders, the IR spectrum shows a new peak ($\approx 460\,cm^{-1}$) attributed to Si–N.

3.3 Annealing experiments

TGA under argon or nitrogen atmosphere coupled with mass spectrometry analysis (TG–MS) is presented elsewhere.[12] Under Ar or N_2 atmosphere the weight loss around 1000°C is correlated to CH_4 release. The experiment under argon atmosphere shows that above 1400°C, the weight loss is correlated to N_2 release.

Figures 3 and 4 present the evolution of the weight loss and the BET surface as a function of the temperature for powders with different C/N composition ($0{\cdot}2 < C/N < 2{\cdot}5$). 'Carbon-rich' powders (HMDS 22, 28), 'nitrogen-rich' powders (HMDS 35,

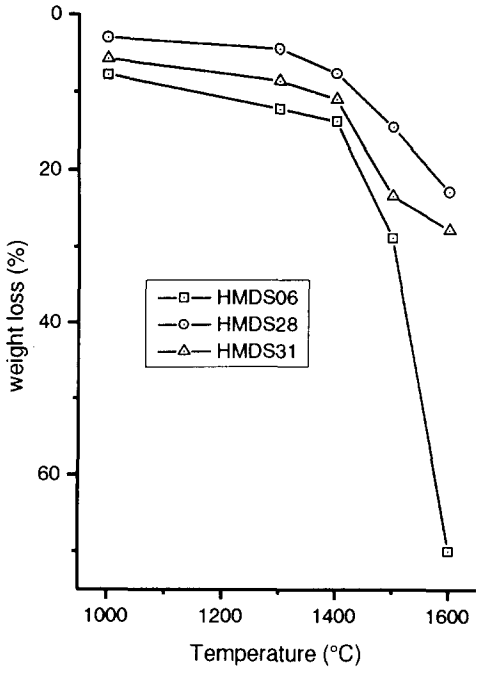

Fig. 3. Weight loss of samples HMDS 06, 28 and 31 as a function of annealing temperature.

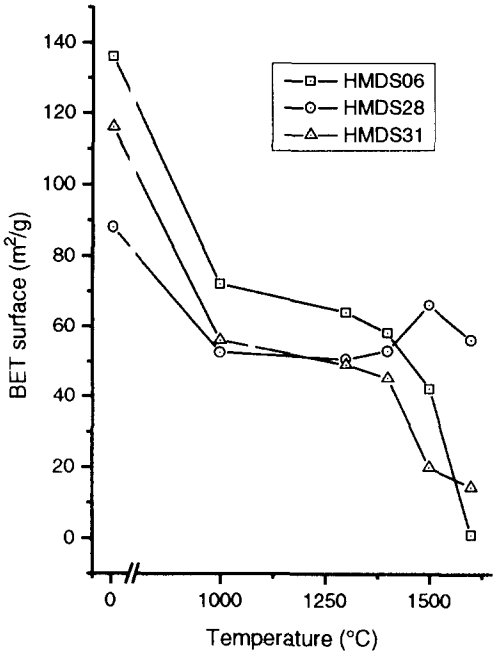

Fig. 4. Evolution of the BET surface of 06, 28 and 31 as a function of annealing temperature.

06) and an 'intermediate' powder (HMDS 31) have been studied. Several points can be noted:

—For all these powders, crystallization occurs between 1400°C and 1500°C.

—After heat treatment at 1000°C, the IR spectra no longer shows hydrogenated structures such as Si–H, Si–CH_3. This is in good agreement with the TG–MS results, which show the release of CH_4 at this temperature.

The detailed results, particular to each powder, are discussed in the following sections.

3.3.1 Carbon-rich powders

TGA under N_2 atmosphere shows a weight loss of 8% and 2% at 1000°C for HMDS 22 and 28 respectively. This is consistent with the IR analysis which shows that HMDS 22 is the most hydrogenated powder. The weight loss is quite small, compared to previous work (10%).[11] The ceramic yield (liquid → powder) after heating at 1000°C is then in the range 31–45%. The weight loss of the HMDS 22 pellet after heat treatment at 1000°C for one hour under N_2 atmosphere is 8%, which is consistent with TGA.

Figures 3 and 4 present the weight loss and the BET surface of HMDS 28 as a function of temperature. The evolution of HMDS 22 is quite similar and is thus not reported on these figures. Up to 1000°C, the BET specific surface decreases (Fig. 4). TEM micrographs show an aggregation of the particles which also show a slight increase in the size.

Between 1000 and 1400°C, the weight of the pellets decreases gently and the BET measurement is quite stable, which indicates that no important chemical or physical changes are taking place in this temperature range.

At 1500°C, a large IR band centred at 890 cm^{-1} indicates the presence of the SiC bond, whereas no bands assignable to the oxidized phase are detected. In addition, a broad band in the XRD diagram demonstrates the beginning of crystallization. The weight loss becomes much higher, while the BET surface suddenly increases (Figs 3 and 4). TEM micrographs show the presence of few crystallized

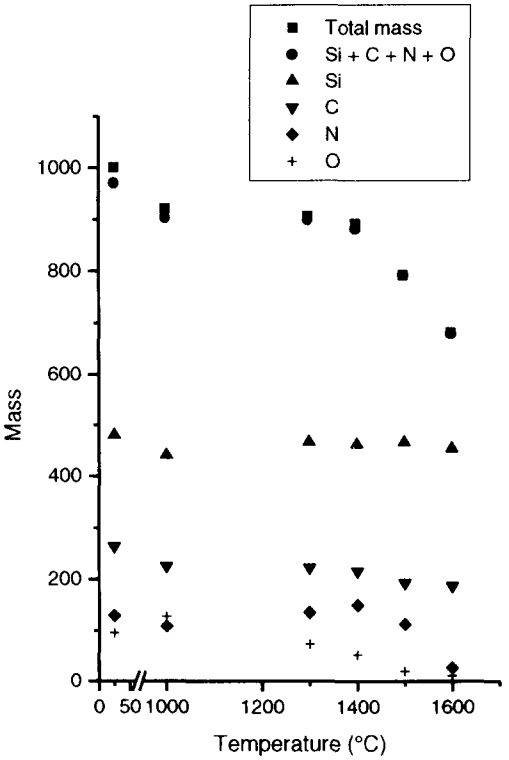

Fig. 5. Evolution of the chemical composition of pellets (HMDS 22) as a function of annealing temperature.

particles but there is no significant evolution of the size. This change in the BET surface may be related to an increase of the porosity.

At 1600°C, the BET surface decreases, indicating the growth of particles as usually observed with increasing temperature. This grain growth is confirmed by the TEM micrograph which shows only crystallized particles. A XRD diagram shows the presence of β-SiC together with α-SiC.

Figure 5 shows the evolution of the weight per chemical element (Si, C, N, O) as a function of annealing temperature, supposing a pellet with an initial weight of 1000 mg. These measurements are consistent with the observations obtained by other methods:

—After heat treatment, no more CH bonds can be identified in the IR spectra. With increasing temperature, the sum Si + C + N + O becomes closer and closer to the total mass of the pellet. This confirms the significant hydrogenation of the as-formed powders and the subsequent dehydrogenation of the powders with heating treatments.

—The powder obtained after heat treatment at 1000°C is more oxidized than the as-formed powder. This can be explained by the release of hydrogenated products during the heat treatment, leaving dangling bonds which are susceptible to oxidation when exposed to air.

—From 1000 to 1400°C, the weight of N in the powder increases. The IR spectrum shows a small peak at 460 cm^{-1} characteristic of the Si–N bond. At these temperatures, flowing N_2 introduced in the furnace can decompose, producing atomic N. This can then be incorporated into the structure of the powders in the position of dangling bonds which remain following dehydrogenation.

—The weight loss after 1400°C, with release of N_2, corresponds to a rapid decrease of N in the pellet. Thermodynamic calculations[14] show that at a nitrogen pressure of 0·1 MPa (atmospheric pressure) and at 1440°C, the following reaction can occur:

$$Si_3N_4(s) + C(s) \rightarrow 3SiC(s) + 2N_2(g) \quad (1)$$

From the chemical composition presented in Table 2, one obtains for HMDS 22 the formula $SiC_{1\cdot28}N_{0\cdot54}O_{0\cdot34}$, which corresponds to a structure containing free C. The experimental observations already described in this section are then in good agreement with reaction (1).

—At 1600°C, the chemical composition of the pellet is close to SiC, coherent with the XRD diagram of the crystallized particles.

—One can also see from chemical analysis (Fig. 5) that no Si is lost during annealing.

—The loss of C begins at 1000°C, in agreement with TG–MS, whereas increasing the temperature increases only very weakly the loss of C.

3.3.2 Nitrogen-rich powders

For the samples HMDS 06 and 35 the weight loss (Fig. 3) is always greater than that observed for carbon-rich powders, as already reported.[12] After 1400°C, the weight loss suddenly increases. The BET

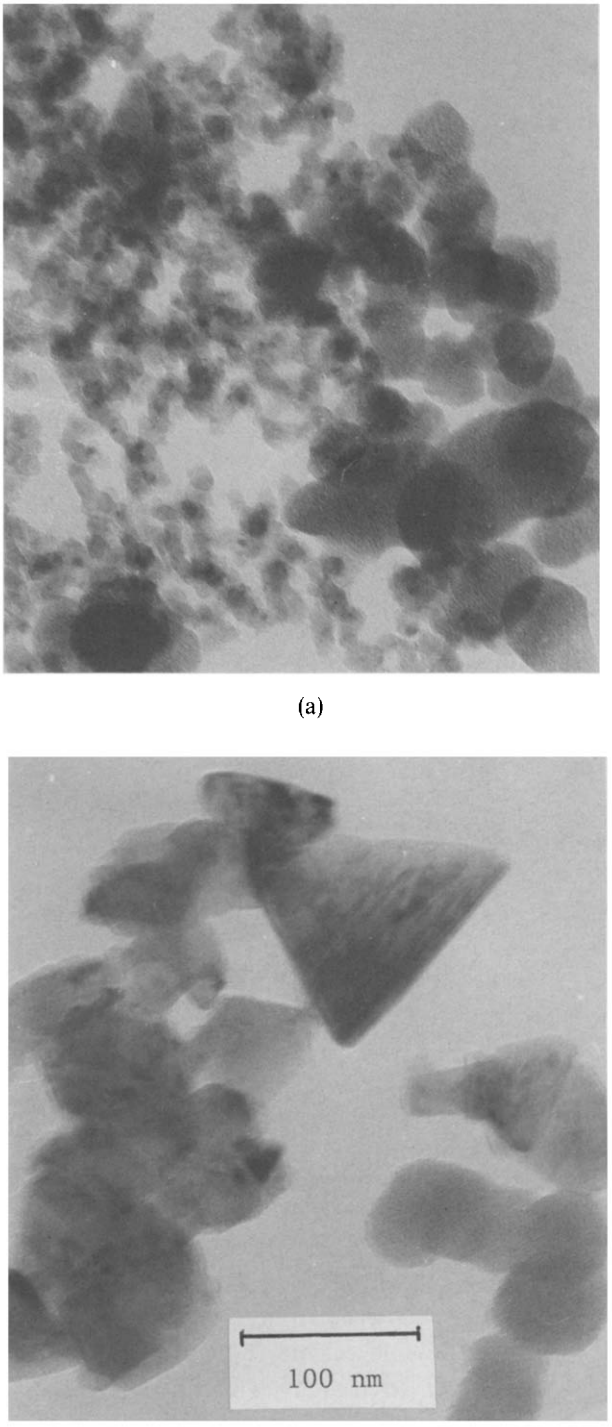

(a)

(b)

Fig. 6. TEM micrographs of HMDS 31 after annealing under nitrogen atmosphere at (a) 1400°C and (b) 1600°C.

surface (Fig. 4) decreases continuously from 1000 to 1600°C, with again a sudden change in the slope at 1400°C. TEM micrographs show a slight evolution in the size of the particles up to 1400°C; the particles become more and more agglomerated. At 1500°C, XRD diagrams show a beginning of crystallization. Crystallized and amorphous particles are present on TEM micrographs. At 1600°C, one observes crystallized particles with an increasing mean size and XRD diagrams show the α-Si_3N_4 structure.

3.3.3 Intermediate powder

The weight loss of HMDS 31 is quite comparable to the one of a C-rich powder (Fig. 3). The BET surface (Fig. 4) decreases continuously from 1000 to 1600°C, which seems more comparable to the N-rich powder, but the growth of particles is more limited. Figure 6 presents the morphology of the powders at 1400 and 1600°C. One can see that the bimodal distribution is still present at 1400°C. Amorphous and crystallized particles are both present after a one-hour treatment at 1600°C. The XRD diagram shows in this case a mixture of SiC and Si_3N_4.

Further studies are necessary to achieve a more complete understanding of the phenomena occurring in these powders, in particular in the range 1300–1500°C (beginning of crystallization). The annealing experiments will be completed using longer dwell duration. New characterization methods, in particular methods sensitive to the local structure, such as MAS–NMR, will be employed.

4 Conclusion

A success in obtaining substantial amounts (at laboratory scale) of pre-ceramic nanophase powders using a safe and relatively low-cost liquid precursor has been reported. The powders are obtained with variable C content (in the range 7–30 wt%) and size. Unfortunately, the process is limited to low viscosity liquids. To scale up the process, the next step is to modify the experimental set up in order to use more viscous precursors which are easily produced at low cost such as polysilazane compounds.

First results about annealing experiments on a C-rich powder have been presented. Also, other samples with different C contents will be studied in order to understand the relations between composition of the pre-ceramic powder, annealing atmosphere and composition of the final product. The ability of these powders for processing into bulk materials, i.e. the ability to sinter, will be tested.

Acknowledgements

This work was supported by the CEC Brite/Euram project 4236/90 'Cost Effective Laser Synthesized Nanoscale Powders and Cases of Thermomechanical Applications'. The authors gratefully acknowledge this support and wish to thank their colleagues L. Boulanger, C. Robert (CEA) and J. P. Disson (Elf-Atochem).

References

1. Komarneni, S., Nanocomposites. *J. Mater. Chem.*, **2**(12) (1992) 1219.
2. (a) Wakai, F., Kodoma, Y., Sakaguchi, S., Murayama, N., Izaki, K. & Niihara, K., A superplastic covalent crystal composite. *Nature*, **344** (1990) 421.
2. (b) Niihara, K. & Nakhira, A., New design concept of structural ceramics, ceramics nanocomposites. *J. Ceram. Soc. Jpn*, **99**(10) (1991) 974.
3. Seyferth, D. & Wiseman, G., High yield synthesis of Si_3N_4/SiC ceramics materials by pyrolysis of a novel polyorganosilazane. *J. Am. Ceram. Soc.*, **67** (1984) C-132.
4. Lee, H., Eguchi, K. & Yoshida, T., Preparation of ultrafine silicon nitride, and silicon nitride and silicon carbide mixed powders in a hybrid plasma. *J. Am. Ceram. Soc.*, **73** (1990) 3356.
5. Suzuki, T., Kawakami, T. & Koyama, T., Fine amorphous powder and process for preparing fine powdery mixture of silicon nitride and silicon carbide, US Patent 4 594 330, 10 June 1986.
6. Xiao, T. D., Gonsalves, K. E., Strutt, P. R. & Klemens, P. G., Synthesis of Si(C, N) nanostructured powders from an organometallic aerosol using a hot wall reactor. *J. Mater. Sci.*, **28** (1993) 1334.
7. Cannon, W. R., Danforth, S. C., Flint, J. H., Haggerty, J. S. & Marra, R. A., Sinterable ceramic powders from laser driven reactions I. Process description and modeling. *J. Am. Ceram. Soc.*, **65** (1982) 324.
8. Cauchetier, M., Croix, O., Luce, M., Baraton, M. I., Merle, T. & Quintard, P., Nanometric Si/C/N composite powders: laser synthesis and IR characterization. *J. Eur. Ceram. Soc.*, **8** (1991) 215.
9. Alexandrescu, R., Morjan, I., Borsella, E., Botti, S., Fantoni, R., Dikonimos, T., Giorgi, R. & Enzo, S., Composite ceramic powders obtained by laser induced reactions of silane and amines. *J. Mater. Res.*, **6**(11) (1991) 2442.
10. Suzuki, M., Maniette, Y., Nakata. Y. & Okutani, T., Synthesis of silicon carbide–silicon nitride composite ultrafine particles using a carbon dioxide laser. *J. Am. Ceram. Soc.*, **76** (1993) 1195.
11. Gonsalves, K. E., Strutt, P. R., Xiao, T. D. & Klemens, P. G., Synthesis of Si(C, N) nanoparticles by rapid laser polycondensation/crosslinking reactions of an organosilazane precursor. *J. Mater. Sci.*, **27** (1992) 3231.
12. Cauchetier, M., Croix, O. M., Herlin, N. & Luce, M., Nanocomposites Si/C/N powders production by laser–aerosol interaction. *J. Am. Ceram. Soc.* (in press).
13. Rice, G. W. & Woodin, R. L., Kinetics and mechanism of laser-driven powder synthesis from organosilane precursors. *J. Mater. Res.*, **4**(6) (1989) 1538.
14. Nickel, K., Hoffmann, M., Greil, P., Petzow, G., Thermodynamic calculations for the formation of SiC-whisker-reinforced Si_3N_4 ceramics. *Adv. Ceram. Mater.*, **3**(6) (1988) 557.